Feeding of the $11/2^-$ isomers in stable Ir and Au isotopes

N. Fotiades,* R. O. Nelson, M. Devlin, S. Holloway, T. Kawano, P. Talou, and M. B. Chadwick
Los Alamos National Laboratory, Los Alamos, New Mexico 87545, USA

J. A. Becker and P. E. Garrett†
Lawrence Livermore National Laboratory, Livermore, California 94550, USA

(Received 29 July 2009; revised manuscript received 18 August 2009; published 23 October 2009)

Excited states in ^{191}Ir, ^{193}Ir, and ^{197}Au were studied and absolute partial γ-ray cross sections were measured using the $(n,n'\gamma)$ reaction. A Compton-suppressed germanium-detector array (GEANIE) for γ-ray spectroscopy was used for the measurement and the broad-spectrum pulsed neutron source of the Los Alamos Neutron Science Center's WNR facility provided energetic neutrons. The energy of the incident neutrons was determined using the time-of-flight technique. Absolute partial γ-ray cross sections were measured up to incident neutron energy of 20 MeV for several transitions feeding directly the $11/2^-$ isomers and ground states in ^{191}Ir, ^{193}Ir, and ^{197}Au. The feeding of the $11/2^-$ isomers, which originate from the odd proton occupying the $h_{11/2}$ orbital, was found for the three targets to be very similar and increasing relative to the feeding of the corresponding ground state with increasing neutron energy up to $E_n \sim 10$ MeV. Above this neutron energy the opening of the $(n,2n)$ reaction channel strongly affects the population of the isomers and leads to a decrease of their relative population compared to the population of the ground states. The experimental results are compared with theoretical predictions from the GNASH reaction model calculation implementing a version of the spin distribution for the pre-equilibrium reaction piece with either a compound nucleus spin distribution (CN-GNASH) or a Feshbach-Kerman-Koonin (FKK-GNASH) quantum mechanical spin distribution. The effects of the spin cutoff parameter values on the population of states are examined. Evidence is presented that FKK-GNASH provides a description of the experimental data that mitigates the need for adjustment of the level density parameter to fit the data.

DOI: 10.1103/PhysRevC.80.044612 PACS number(s): 25.40.Fq, 24.10.−i, 27.80.+w, 28.20.−v

I. INTRODUCTION

Cross sections of (n,xn) reactions are necessary in applications, e.g., activation detectors (also known as radiochemical detectors) used to probe energy components of a neutron fluence. The ^{191,193}Ir isotopes constitute a set of such detectors: the few-MeV region can be probed by the (n,n') production of the $11/2^-$ isomer [1] of ^{193}Ir($T_{1/2} = 10.53d$), whereas the higher-energy part of the spectrum can be assessed through (n,xn) reactions $(x = 2, 3)$ on both ^{191,193}Ir leading to the long-lived isotopes ^{189,190,192}Ir [2].

The $11/2^-$ isomer of ^{193}Ir originates from the odd proton occupying the $h_{11/2}$ orbital and has been observed also in ^{191}Ir($\tau = 4.94s$) [3] and the stable isotope ^{197}Au($\tau = 7.73s$) [4]. In fact, the nuclear structure of all these three isotopes is similar at low-excitation energies [5], the lowest negative-parity state being the $11/2^-$ isomer. Moreover, the sequence of negative-parity states above the isomers is also similar and originates from the proton decoupled band built on the $h_{11/2}$ orbital [6]. For each target, four γ rays are observed which feed the isomers directly in (n,n') reactions.

Partial γ-ray cross sections for low-lying states (in particular the 2^+ to 0^+ ground-state transitions in even-even nuclei) often can be used to infer reaction channel cross sections accurately because a very large fraction of all γ-ray decays pass through the 2^+ first-excited state (see, for instance, Ref. [7]). For more complicated cases, in which the decay scheme involves many more levels, nuclear reaction model calculations were tested and combined with the measured γ-ray data to infer more accurate (n,xn) cross sections (see, for instance, Ref. [8]). The odd-mass nuclei of ^{191}Ir, ^{193}Ir, and ^{197}Au are complicated cases compared to even-even nuclei. In 1996 an initiative was taken to extend such studies to other nuclei and the data reported here are part of this program of measurements which use the Germanium Array for Neutron-Induced Excitations (GEANIE) [9]. Results from other similar studies (both with GEANIE and before GEANIE) include data taken on samples of ^{207,208}Pb [8], ^{27}Al [10], ^{196}Pt [11–13], ^{48}Ti [14,15], ^{92}Mo [16,17], ^{89}Y [18], ^{90}Zr [18,19], ^{150}Sm [20], ^{239}Pu [21], ^{238}U [22], and ^{235}U [23]. For this effort Ge and BGO detectors of the former HERA spectrometer at LBNL [24] were transferred to LANL for a joint LANL/LLNL project. Eleven new planar-geometry Ge detectors were added to the new GEANIE spectrometer [9] and escape-suppression shields were used to reduce backgrounds. All of the results obtained provide a database which is useful for many purposes including testing nuclear reaction model calculations in detail. These data provide information on nuclear reactions and structure and have many applications in technology, such as radiation transport calculations and radiochemical detector refinements.

In the present work, γ-ray energies were measured with high precision, and absolute partial cross sections as a function of incident neutron energy for production of these γ rays were determined at the Los Alamos Neutron Science Center (LANSCE) Weapons Neutron Research (WNR) facility [25]

*fotia@lanl.gov
†Present address: Physics Department, University of Guelph, Guelph, Ontario, N1G 2W1 Canada.

in three different experiments (one for each nuclide, ^{191}Ir, ^{193}Ir, and ^{197}Au). The range of neutron energies was from threshold to 20 MeV. Partial results from the experiments described here have also been reported in Refs. [6,26]. New levels in ^{197}Au were reported in Ref. [6].

In a previous paper the use of the Feshbach-Kerman-Koonin (FKK) theory in the GNASH nuclear reaction model code was shown to give an improved description of inelastic scattering in ^{48}Ti where pre-equilibrium processes are important [14]. In particular, high-spin state population by inelastic scattering is better described, requiring no *ad hoc* adjustment of the level density parameter. Of special interest here are the cross sections of the four well-resolved individual γ rays feeding directly the $11/2^-$ isomers of ^{191}Ir, ^{193}Ir, and ^{197}Au, because they enable a study of spin effects in reaction model calculations, such as with GNASH, that includes compound, pre-equilibrium, and direct mechanisms. These results extend the FKK GNASH calculations to heavier, odd-mass nuclides with good results.

II. EXPERIMENTS

The γ rays produced in the bombardment of the ^{191}Ir, ^{193}Ir, and ^{197}Au targets by neutrons were observed with the GEANIE spectrometer [9]. GEANIE is located 20.34 m from the WNR spallation neutron source on the 60R (60°-right) flight path. The neutrons were produced in a ^{nat}W spallation target driven by an 800 MeV proton beam with a time structure that consists of 625 μs-long "macropulses," with each macropulse containing sub-nanosecond-wide "micropulses," spaced every 1.8 μs(^{197}Au experiment) or 3.6 μs(^{191}Ir and ^{193}Ir experiments). The energy of the neutrons was determined using the time-of-flight technique. GEANIE is comprised of 11 Compton suppressed planar Ge detectors (low-energy photon spectrometers—LEPS), nine Compton suppressed coaxial Ge detectors, and six unsuppressed coaxial Ge detectors.

The ^{191}Ir target consisted of one thin-walled polystyrene capsule, 2.3 cm in diameter, containing 2.0 g of Ir metal powder, 98.2% enriched in ^{191}Ir (areal density 0.54 g/cm^2). In the ^{193}Ir experiment 2.0 g of Ir metal powder, 99.6% enriched in ^{193}Ir, were tightly encapsulated in a polystyrene capsule 1.3 cm in diameter and 0.34 cm thick (areal density 1.58 g/cm^2). Polystyrene was chosen for the capsule material because it does not contain fluorine or chlorine which produce strong γ-ray backgrounds when irradiated by neutrons. Finally, the ^{197}Au target consisted of one foil, 1.43 g/cm^2 thick. Two 0.05 mm natural Fe foils were placed on the front of the targets during part of the experiments and in the case of the ^{197}Au experiment two more foils were added on the back of the ^{197}Au target. The Fe foils were included so that the known cross section at $E_n = 14.5$ MeV [27] of the strong 846.8-keV, $2^+ \rightarrow 0^+$ transition of ^{56}Fe, produced in natural Fe from inelastic scattering, could be used to normalize the cross sections obtained in the present experiments.

The neutron flux on target was measured with a fission chamber, consisting of ^{235}U and ^{238}U foils [28], located 18.5 m from the center of the spallation target. Detector efficiencies were determined using a variety of calibrated γ-ray reference sources (^{60}Co, ^{137}Cs, ^{152}Eu, and ^{241}Am). Data acquisition system "dead-times" were measured by comparing the raw Ge-detector counts with recorded Ge-detector pulse-height spectrum counts. During the experiment the event data were stored for subsequent offline analysis. A total of $\sim 8.5 \times 10^8$, $\sim 4 \times 10^8$, and $\sim 1.1 \times 10^9$ singles and higher-fold data were recorded in the ^{191}Ir, ^{193}Ir, and ^{197}Au experiments, respectively.

III. EXPERIMENTAL RESULTS

Prior to the present work there were no experimental measurements of the population of the ^{191}Ir^m and ^{197}Au^m $11/2^-$ isomers via (n,n') reactions, while the isomer population cross section in the ^{193}Ir$(n,n')^{193}$Ir^m reaction has one experimental measurement available [2]. This was a foil activation measurement obtained for four incident neutron energies at 7.57, 8.59, 9.34, and 14.7 MeV.

Four strong transitions were observed in our data to directly populate the $11/2^-$ isomers in ^{191}Ir, ^{193}Ir, and ^{197}Au. Partial level schemes of ^{191}Ir, ^{193}Ir, and ^{197}Au showing these transitions are shown in Fig. 1 and the information on all these

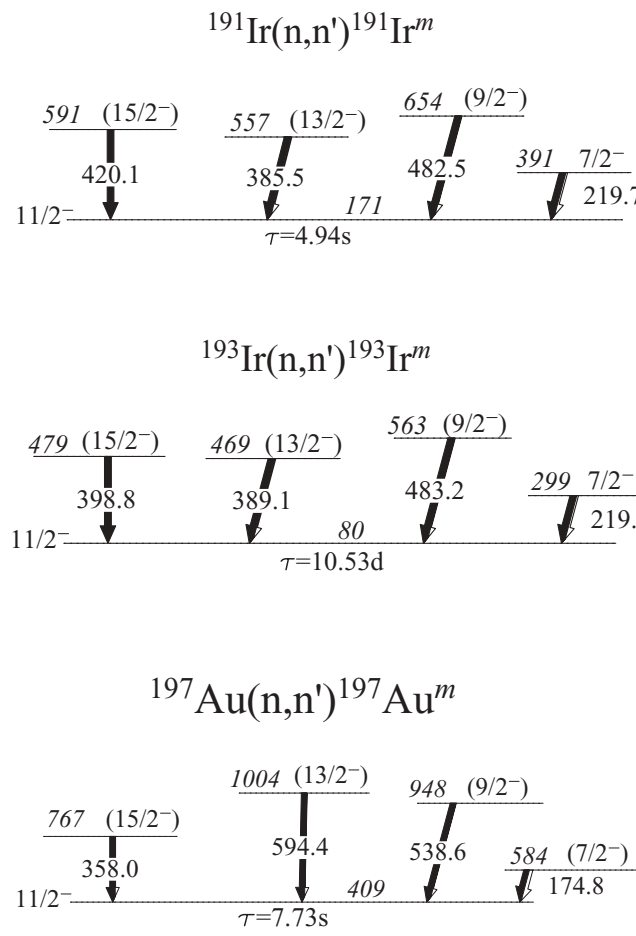

FIG. 1. Partial level schemes showing the transitions of ^{191}Ir, ^{193}Ir, and ^{197}Au relevant to the present work. All γ-ray and level energies are given in keV. The white portion of the arrows indicates the fraction of the decay that is internally converted. Levels and half-lives were taken from Refs. [1,3,4,6].

TABLE I. γ-ray energy, initial level excitations, spins and parities, half-life, intensity, multipolarity, and internal conversion coefficient for all transitions in Fig. 1. The final levels for all transitions are the $11/2^-$ isomers in Fig. 1. All information for levels and transitions were adopted from Refs. [1,3,4,6]. Multipolarities and conversion coefficients in parentheses have not been experimentally determined.

E_γ (keV)	E_i (keV)	J_i^π	$T_{1/2}$	I_γ	Multipolarity	α
			^{191}Ir			
219.7	391	$\frac{7}{2}^-$	240 ps	100	$E2$	0.256
385.5	557	$(\frac{13}{2}^-)$		100	$(M1)$	(0.148)
420.1	591	$(\frac{15}{2}^-)$		100	$(E2)$	(0.037)
482.5	654	$(\frac{9}{2}^-)$		66	$(M1)$	(0.081)
			^{193}Ir			
219.2	299	$\frac{7}{2}^-$	0.19 ns	100	$E2$	0.257
389.1	469	$(\frac{13}{2}^-)$		100	$(M1)$	0.145
398.8	479	$(\frac{15}{2}^-)$		100	$(E2)$	0.0428
483.2	563	$(\frac{9}{2}^-)$		63	$(M1)$	0.0814
			^{197}Au			
174.8	584	$(\frac{7}{2}^-)$		100	$(E2)$	(0.61)
358.0	767	$(\frac{15}{2}^-)$		100	$(E2)$	(0.062)
538.6	948	$(\frac{9}{2}^-)$		61	$(M1)$	(0.0725)
594.4	1004	$(\frac{13}{2}^-)$		100	$(M1)$	(0.056)

γ rays is summarized in Table I. The absolute cross sections observed for these transitions are shown in Figs. 2, 3, and 4. The excitation functions for the corresponding transitions in the three targets are very similar, as can be seen in Figs. 2, 3, and 4, but there are differences in the absolute cross section values. However, the sum of the cross sections obtained for the four transitions (see Fig. 5) for each target is similar in shape and magnitude and is expected to represent a large portion of the reaction cross section that populates the corresponding isomers, since these transitions are emitted by the lowest states of the decoupled band built on the proton-hole $h_{11/2}$ configuration for which the $11/2^-$ isomers are the band-heads.

In the ^{197}Au experiment the 1.8 μs "micropulse" spacing resulted in "frame overlap" issues in which the time overlap of high-energy neutrons of one pulse with lower-energy neutrons of the previous pulse may result (depending on the reaction threshold) in measurement of cross sections summed for two incident neutron energies. In the case of the Au data, neutrons below $E_n \sim 650$ keV and at $E_n > 145$ MeV (plus the gamma flash from the neutron production target) could not be separated. Because of the frame overlap and for convenience of the analysis, in Fig. 4 we report the cross sections only for incident neutron energies $E_n > 1$ MeV. The use of 3.6 μs "micropulse" spacing in the ^{191}Ir and ^{193}Ir experiments eliminated this issue for the data in Figs. 2 and 3 where analysis extends to the reaction threshold.

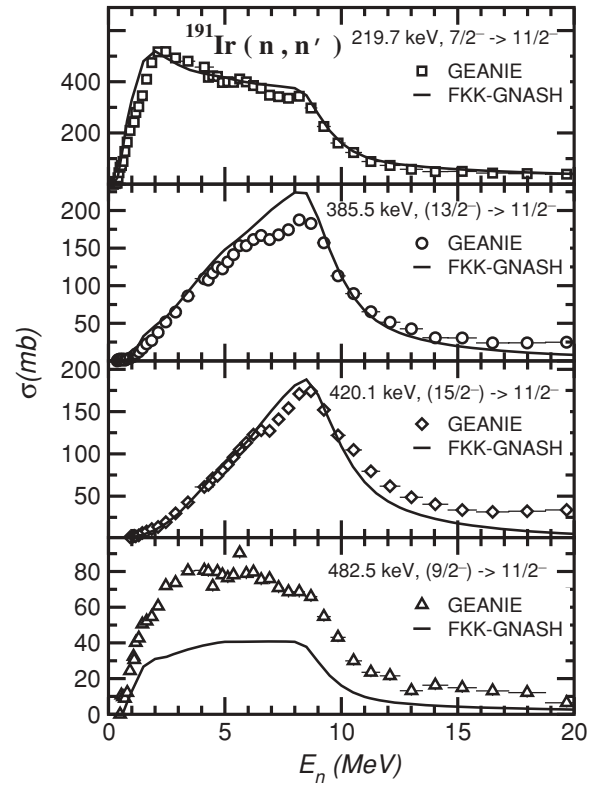

FIG. 2. Cross sections obtained for the four transitions feeding directly the $11/2^-$ isomer as a function of incident neutron energy in the ^{191}Ir experiment. Specifically, these transitions [3] are 219.7 keV, $7/2^- \rightarrow 11/2^-$ transition from 391-keV level (squares), 482.5 keV, $(9/2^-) \rightarrow 11/2^-$ transition from 654-keV level (triangles), 385.5 keV, $(13/2^-) \rightarrow 11/2^-$ transition from 557-keV level (circles), and 420.1 keV, $(15/2^-) \rightarrow 11/2^-$ transition from 591-keV level (diamonds). The solid lines are FKK-GNASH model calculations (see text).

All experimental cross sections reported in the present work were corrected for γ-ray attenuation in the sample, internal conversion, and the contribution from neutrons produced by scattering and reactions in the targets. The latter correction was done by simulating the neutron flux produced inside the targets for all incident neutron energies using the Los Alamos Monte Carlo code MCNPX [29]. The multiple scattering and reaction calculations follow the method described in Ref. [30]. These corrections tend to be largest at higher incident neutron energies and for lower threshold reactions, and are dependent on the sample thickness. The maximum correction for multiple scattering and reactions was a reduction of the measured cross section by 35% at $E_n = 20$ MeV. A large part of this correction is due to lower energy neutrons emitted in (n,xn) reactions. These neutrons may have a large cross section for γ-ray production [depending on the (n,n') cross section] but are produced essentially simultaneously with γ rays from higher energy neutrons that have a much smaller cross section for γ-ray production. Contributions from charged particles are ignored in this process due to their generally smaller production cross sections and shorter path lengths. All experimental cross-section values reported in the present work

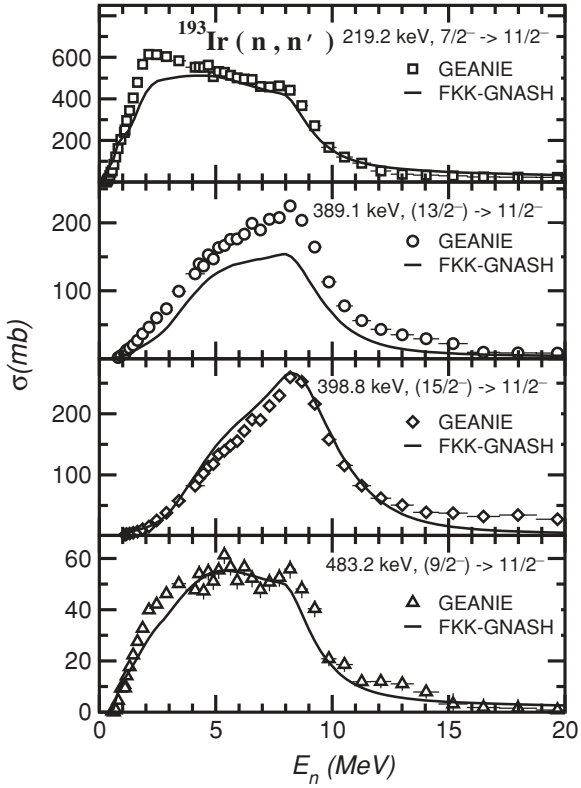

FIG. 3. Cross sections obtained for the four transitions feeding directly the $11/2^-$ isomer as a function of incident neutron energy in the ^{193}Ir experiment. Specifically, these transitions [1] are 219.2 keV, $7/2^- \rightarrow 11/2^-$ transition from 299-keV level (squares), 483.2 keV, $(9/2^-) \rightarrow 11/2^-$ transition from 563-keV level (triangles), 389.1 keV, $(13/2^-) \rightarrow 11/2^-$ transition from 469-keV level (circles), and 398.8 keV, $(15/2^-) \rightarrow 11/2^-$ transition from 479-keV level (diamonds). The solid lines are FKK-GNASH model calculations (see text).

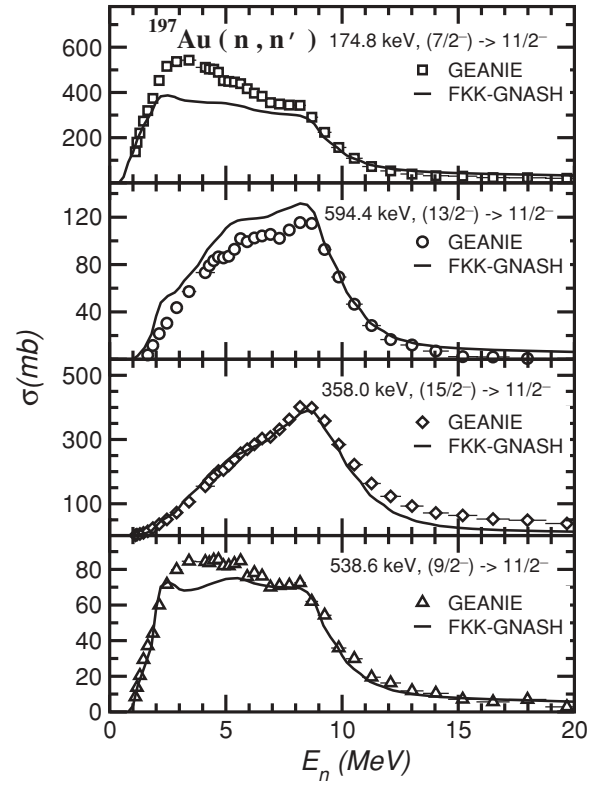

FIG. 4. Cross sections obtained for the four transitions feeding directly the $11/2^-$ isomer as a function of incident neutron energy in the ^{197}Au experiment. Specifically, these transitions [6] are 174.8 keV, $(7/2^-) \rightarrow 11/2^-$ transition from 584-keV level (squares), 538.6 keV, $(9/2^-) \rightarrow 11/2^-$ transition from 948-keV level (triangles), 594.4 keV, $(13/2^-) \rightarrow 11/2^-$ transition from 1004-keV level (circles), and 358.0 keV, $(15/2^-) \rightarrow 11/2^-$ transition from 767-keV level (diamonds). The solid lines are FKK-GNASH model calculations (see text).

have been submitted to the CSISRS database at the National Nuclear Data Center at Brookhaven National Laboratory.

Systematic uncertainties for the data reported here include: (a) overall normalization uncertainties from uncertainties in sample thickness (∼1%), in the Fe foil thickness (∼1%), and in the system dead times (∼1%); (b) γ-energy dependent systematic uncertainties from the uncertainties in the detector efficiency (∼5%), γ-ray absorption corrections (∼1%) and internal conversion corrections (∼0.1%); and (c) neutron-energy-dependent systematic uncertainties from the neutron flux measurement (∼8%) [this includes both statistical and systematic components including uncertainties in the Fe(n,$n'\gamma = 847$ keV) cross section and detection efficiency] and from the multiple scattering and reactions correction (0% at threshold to ∼15% at $E_n = 20$ MeV). The combined systematic uncertainties are estimated to range from 8% for $1 < E_n$ (MeV) < 8, increasing to ∼20% at $E_n = 20$ MeV.

IV. THEORETICAL CALCULATIONS

GNASH calculations [31], which utilize the Hauser-Feshbach compound nucleus theory (HF), were performed to obtain γ-ray production cross sections for the four dominant transitions feeding the $11/2^-$ isomer of ^{191}Ir, ^{193}Ir, and ^{197}Au. In HF, a projectile incident on a target produces a compound nucleus (CN) which is regarded as long enough lived to have reached equilibrium. As such, the properties of the CN do not depend on the reaction that produced it but only on conserved quantities such as energy, spin, and parity. As the decay of the CN is independent of how the CN was formed, the reaction cross section can be factorized into the cross section for the formation of the CN by the initial channel and the probability of decay to the final reaction channel. Explicitly, the cross section for a general reaction $X(a, a')Y$ is given by

$$\sigma_{a,a'}(\epsilon, I, P; E', I', P') = \sum_{J,\pi} \sigma_a(\epsilon, I, P; E_x, J, \pi) \times \frac{\Gamma_{a'}(E_x, J, \pi; E', I', P')}{\Gamma(E_x, J, \pi)}, \quad (1)$$

where (ϵ, I, P) are the center-of-mass energy, spin, and parity of the projectile, (E', I', P') are the energy, spin, and parity of the final channel nucleus, and (E_x, J, π) the excitation energy, spin, and parity of the CN. The probability of decay to the final channel is given as the ratio of the partial width for decay, $\Gamma_{a'}$

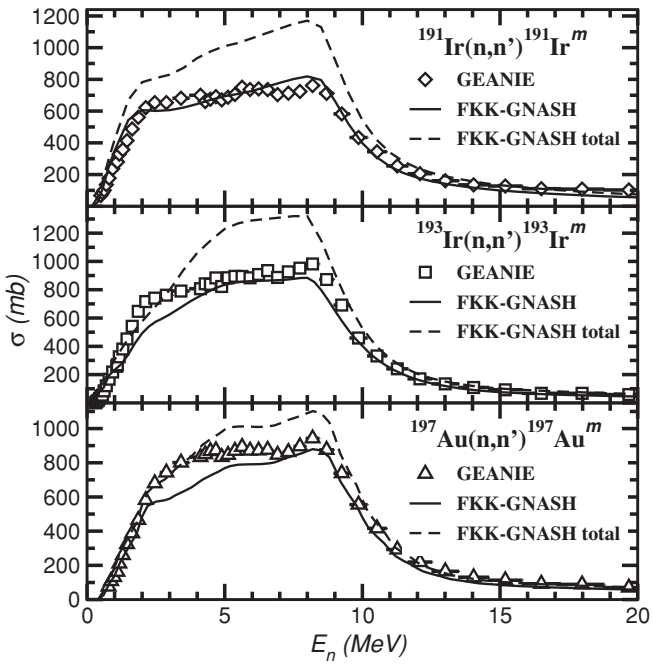

FIG. 5. Sums of cross sections (symbols) obtained for the four transitions feeding directly the $11/2^-$ isomers in ^{191}Ir, ^{193}Ir, and ^{197}Au (see Fig. 1) compared with the corresponding FKK-GNASH predictions (solid lines). The dashed lines are the FKK-GNASH predictions for the total production of the isomers.

and Γ the total width for all possible decays. The formation cross section and decay probability can be expressed in terms of optical model transmission coefficients, $T_{\ell_j}(E)$ which are calculated externally (using, for example, ECIS) and provided as input to GNASH.

From equilibrium, the CN decays via a series of γ and particle emissions. Through each step of the CN decay, GNASH calculates detailed level populations for each nuclear state present in the decay chain. The population of the initial levels in the first CN is given by

$$\mathcal{P}^{(1)}(E_x, J, \pi) = \sigma_a(\epsilon, I, P; E_x, J, \pi)\delta(E_x - \epsilon - B_a), \quad (2)$$

where B_a is the binding energy of the projectile. Subsequent populations are determined by

$$\mathcal{P}^{(n+1)}(E_x', J', \pi') = \rho^{(n+1)}(E_x', J', \pi') \sum_{J,\pi} \int_{E_x'+B_{a'}}^{E_x^{max}} dE_x \mathcal{P}^{(n)}(E_x, J, \pi) \times \frac{\Gamma_{a'}^{(n)}(E_x, J, \pi; E_x', J', \pi')}{\Gamma(E_x, J, \pi)}, \quad (3)$$

where $\rho^{(n+1)}(E_x', J', \pi')$ denotes the nuclear level density and E_x^{max} is the maximum excitation energy attainable in the n^{th} compound nucleus. Equation (3) applies to levels in the continuum. Once the compound nucleus is fully de-excited, these populations determine all relevant γ-ray and particle emission cross sections.

Despite its relative simplicity, HF has proven to be a suitable model when the composite nucleus is in equilibrium. However, it is well-known that corrections must be incorporated which account for particle emission prior to the composite system coming to equilibrium. GNASH incorporates several corrections to HF which include direct, inelastic cross sections from discrete states calculated using coupled-channels theory. In addition, pre-equilibrium emission occurring at high energies is accounted for using either a semiclassical exciton model or, more recently, the quantum mechanical theory of Feshbach-Kerman-Koonin [32] (FKK). Gamma production cross sections are quite sensitive to the method employed to obtain the pre-equilibrium contribution [15].

A. GNASH Calculations for ^{197}Au

We focus on the calculation details for the ^{197}Au reaction cross sections here. FKK-GNASH calculations of ^{191}Ir are presented in Ref. [33], as well as ^{193}Ir cross sections calculated using the semiclassical exciton model. More recent ^{193}Ir cross section evaluations, obtained using FKK, are provided in Ref. [34]. The FKK-GNASH ^{197}Au cross sections given in Fig. 4 have not been reported previously and therefore more details of the models and parameters used for this calculation follow.

Transmission coefficients for the HF calculations of ^{197}Au were obtained using optical model calculations. Coupled-channels optical potential parameters were taken from Ref. [35]. The γ-ray strength functions (or transmission coefficients) were approximated using the Kopecky and Uhl formalism [36] which utilizes a general Lorentzian form for the $E1$ strength functions. $E2$ and $M1$ strength functions were also included using giant dipole resonance methods. All well-described low-energy discrete nuclear level structure for $^{195-198}$Au were incorporated, including results from the present experiment which significantly improve the level structure of ^{197}Au [6]. The level density model of Ignatyuk *et al.* [37] was used to approximate the high-energy continuum of excited nuclei. Level density parameters are obtained by matching of the discrete and continuum regions. This matching is treated automatically by GNASH and the "default" values were found to be suitable. Pre-equilibrium corrections were calculated using the first step of a multistep FKK model. The calculation procedure is described in Ref. [34]. In addition, width fluctuation corrections, calculated using the Moldauer expression [38], have been included.

The FKK-GNASH calculations of γ-ray production cross sections are given by the solid lines in Figs. 2, 3, and 4. There is reasonable agreement between experiment and theory. The cross sections from "high-spin" excited states, $[(15/2^-) \rightarrow 11/2^-$ and $(13/2^-) \rightarrow 11/2^-]$ are very well reproduced. These transitions are significantly affected by the residual nucleus spin distributions, which we find are best predicted by the FKK pre-equilibrium model. The production cross sections from "low-spin" excited states, $[(7/2^-) \rightarrow 11/2^-$ and $(9/2^-) \rightarrow 11/2^-]$ in some cases are underestimated for incident neutron energies between about 2-7 MeV while for higher incident neutron energies ($E_n > 10$ MeV), these GNASH calculations are somewhat larger than the data for the $[(7/2^-) \rightarrow 11/2^-]$ transitions and somewhat smaller than the data for the other transitions. The summed cross sections shown in Fig. 5 generally agree well with the summed GNASH

calculations. The differences for individual γ rays observed at higher energies tend to average toward the measured cross sections when summed.

B. Spin distributions and level density parameters

The total spin distribution of the initial residual nucleus after neutron inelastic scattering, but before γ-ray cascading, is a sum of pre-equilibrium and compound reaction contributions:

$$R(J) = f(E_x)R_{PE}(J) + [1 - f(E_x)]R_{CN}(J). \quad (4)$$

In GNASH, the fraction of pre-equilibrium emission, $f(E_x)$, is calculated with the exciton model. The J-dependent spin distribution for the pre-equilibrium and compound processes, R_{PE} and R_{CN}, are expressed as

$$R_X(J) = \frac{J+1/2}{\sigma_X^2} \exp\left\{-\frac{(J+1/2)^2}{2\sigma_X^2}\right\}, \quad x = PE \text{ or } CN, \quad (5)$$

where σ_X^2 is the spin cut-off parameter. For the pre-equilibrium process σ_{PE}^2 is different from that of the compound process σ_{CN}^2.

Since σ_{PE}^2 is smaller than σ_{CN}^2, population of high-spin states in a continuum is suppressed when the pre-equilibrium contribution becomes larger. Many nuclear reaction codes, like GNASH or STAPRE usually implicitly assume that the spin distribution in the pre-equilibrium process is the same as the compound process $\sigma_{PE}^2 = \sigma_{CN}^2$, because the classical exciton model cannot give the J-dependence in a rigorous way (though various semiclassical approximations have been made to estimate the effects [39]). The spin distribution in a continuum is determined by the level density spin distribution and the ℓ-dependence of the transmission coefficients $T_{\ell j}$ for incident and out-going channels. In GNASH the spin-cutoff parameter σ^2 of the level density is calculated based on the Gilbert-Cameron formula [40]

$$\sigma^2 = g\langle m^2\rangle T, \quad (6)$$

where g is the single particle state density, $\langle m^2\rangle$ is the mean square value of the angular momentum projection for the single-particle state, and T is the nuclear temperature. Note that the σ's in Eqs. (5) and (6) are different. Equation (5) is for the population and Eq. (6) is for the level density. When $\langle m^2\rangle = 0.24A^{2/3}$ is assumed [41], together with the relation $g = 6a/\pi^2$ and $aT^2 = U$, we obtain

$$\sigma^2 = 0.146\sqrt{aU}A^{2/3}, \quad (7)$$

where U is the nuclear excitation energy corrected by a pairing energy Δ as $U = E_x - \Delta$, and a is the level density parameter. Assuming $g\langle m^2\rangle = \mathcal{I}$, where $\mathcal{I}$ is the moment of inertia, Eq. (6) becomes

$$\sigma^2 = \frac{\mathcal{I}}{\hbar^2}T = 0.0139\sqrt{U/a}A^{5/3}, \quad (8)$$

which is often used in the back-shifted Fermi-gas model [42]. In the approximation that $a \sim A/8$, this becomes similar to Eq. (7) with a slightly smaller constant.

Both expressions of σ^2 tend to overestimate experimentally observable quantities. Analysis of spin distributions at low excitation energies imply that one-half times the value of σ^2 in Eq. (8) gives better agreement with the distribution of low-lying states [43]. In Ref. [44] it is reported that a small reduction in the value from Eq. (8) gives a better fit to the data. A similar tendency is reported in Refs. [45,46]. Also, it has been reported [47] that about 1/4 of the value from Eq. (8) gives a better agreement with the experimental data of isomeric cross section ratios in the α and ^{3}He induced reactions on Hg and Au. This reduction factor is scattered from 0.25 to 1.0, and a possible reason is that σ^2 also depends on the value of the level density parameter a that is used.

Equation (7) is adopted to calculate σ^2 in the GNASH code. The parameter σ^2 has only a small effect on cross sections for lower spins states, but a large effect on cross sections for levels fed by higher-J level densities in the continuum. As shown in Ref. [47], smaller values of σ^2 give lower production cross sections for high-spin isomers. In Ref. [48] it is shown that the isomeric ratio in the ^{196,198}Hg$(n,2n)$ reactions requires a σ^2 value ~15–20% of the value from Eq. (8). Because the pre-equlibrium spin transfer has been treated in only an approximate way in Ref. [48], it is not clear if this reduction of σ^2 is indeed physical. Calculations using the FKK treatment of the spin distribution used here do not indicate a need for a reduced value of σ^2.

We contrast calculations utilizing FKK, and Eq. (7) for σ^2, with calculations using the more usual assumption of the same spin distribution for compound and pre-equilibrium processes coupled with a reduced σ^2 for the case of the ^{193}Ir 398.8 keV γ-ray. Figure 6 shows our measured data

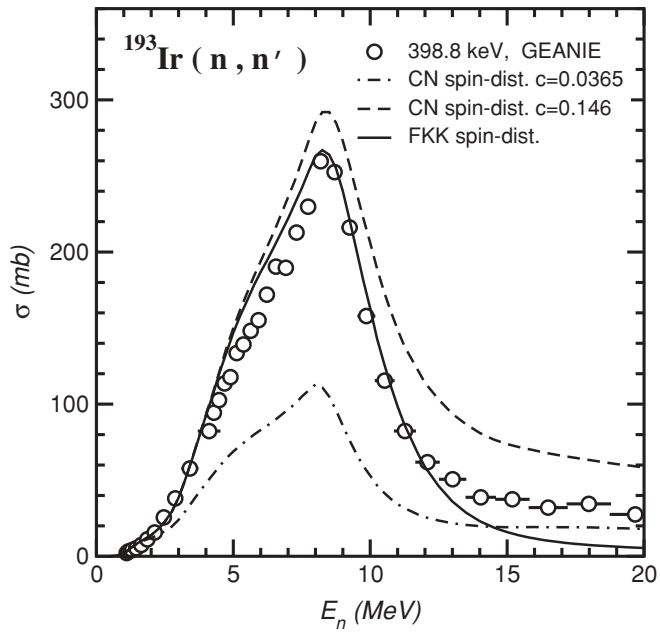

FIG. 6. Comparison of calculated production cross section for the 398.8 keV γ-ray in the ^{193}Ir(n,n') reaction with experimental data. The solid line is the result of FKK-GNASH calculation, the dashed line is a usual GNASH calculation (the same spin distribution for compound and pre-equilibrium processes—also referred to as CN-GNASH), and the dot-dashed line is the same as the dashed line but the spin-cutoff parameter in the level density formula is reduced by a factor of 1/4.

and calculated production cross sections for the 398.8 keV transition in the ^{193}Ir(n,n') reaction. The dashed line is for a single spin distribution with $\sigma^2 = 0.146$. This calculation gives greater cross sections at incident neutron energies above 10 MeV, where pre-equilibrium processes are important. If σ^2 is reduced by a factor of 0.25, the result is the dash-dot curve in Fig. 6 that clearly does not reproduce the measured cross sections. The solid line in Fig. 6 shows the FKK-GNASH calculation using $\sigma^2_{CN} = 0.146$ and σ^2_{PE} obtained using the FKK formalism. Agreement with the data is good at lower neutron energies, while this calculation results in cross sections that are smaller above 13 MeV. Although in Fig. 6 above $E_n = 13$ MeV the FKK-GNASH underestimates the experimental results by about the same factor as the CN-GNASH overestimates them, other recent studies [15] support the case that FKK-GNASH better represents the underlying physics.

V. DISCUSSION

An intercomparison of the sum of cross sections obtained for the four stronger transitions directly populating the $11/2^-$ isomers is shown in Fig. 5. The partial cross section exhibits a similar behavior as a function of incident neutron energy in all three experiments. These sums represent a fraction of the total population of the channels and need to be corrected for the strength of weak or unknown transitions that are not observed in order to deduce the total population. This can be done by using a nuclear reaction model (such as GNASH described in the previous section) to calculate the same quantities, i.e., the sum of the cross sections for the four individual γ rays, along with the total isomer population cross section. The ratio of these quantities can then be used to deduce a reaction channel cross section. Such a procedure was applied in the results of the ^{193}Ir experiment and was reported elsewhere [34,49,50]. However, in this earlier work [50] the spin distributions were assumed to have the compound nucleus spin distribution and did not include FKK spin distributions. Ref. [50] was able to reproduce the γ rays feeding the ^{193}Ir isomer by assuming additional, experimentally unobserved, high-spin states. We note here that the total predicted isomer production from FKK-GNASH for ^{193}Ir$(n,n'\gamma)^{193}$Ir^m, shown as the dashed line in Fig. 5, differs slightly from the corresponding cross section adopted in the latest evaluation [51].

The sum of the cross sections feeding the $11/2^-$ isomer shown in Fig. 5 was divided by the sum of the cross sections obtained for the transitions that feed directly the ground states of ^{191}Ir, ^{193}Ir, and ^{197}Au at each neutron energy. The result is shown in Fig. 7. The sum of the cross sections for the transitions that feed directly the ground states of ^{191}Ir and ^{193}Ir was reported previously (see Fig. 2 in Ref. [26], and discussion therein), and for ^{197}Au the result is very similar. These ratios are similar to isomer ratios but are expected to be missing some fraction of the prompt ground-state-decay cross sections, a fraction that varies with energy. Thus, "pseudo-isomer ratios" can be obtained for cases that can not be measured with activation techniques. The ratios in Fig. 7 exhibit striking similarities in all three experiments. Specifically, at low

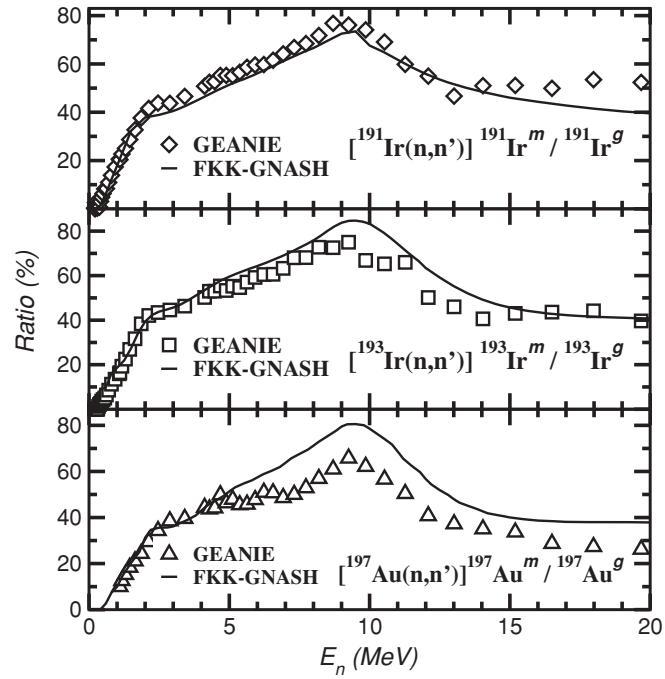

FIG. 7. Ratios of sums of cross sections obtained for the four transitions feeding directly the $11/2^-$ isomers in ^{191}Ir, ^{193}Ir, and ^{197}Au (see Fig. 5) over the sums obtained for the transitions observed to feed directly the ground states of the corresponding isotopes in the respective experiments (see text) compared with the corresponding FKK-GNASH predictions (lines).

neutron energies ($E_n < 1.5$ MeV) the high-spin $11/2^-$ isomer is populated very weakly in all three reactions. However, as the incident neutron energy and hence the angular momentum increases, the population of the $11/2^-$ isomer increases relative to the population of the ground state, a low-spin state [1,3,4] in all three cases. This increase in isomer population continues up to $E_n \sim 10$ MeV. The $(n,2n)$ reaction channel opens up at $E_n \sim 8$ MeV; beginning at neutron energies about 2 MeV above the $(n,2n)$ reaction threshold, the relative population of the isomer decreases suggesting that the opening of the $(n,2n)$ reaction channel affects more the population of the high spin states in the (n,n') channel. The $(n,2n)$ reaction channel proceeds through a compound nucleus formation, with its greater population of the high-spin states in the residual nucleus. The opening of the $(n,2n)$ reaction channel removes angular momentum from the compound system and reduces the population of high-spin isomers in the (n,n') reaction.

The striking similarities in the excitation functions of the corresponding four transitions that feed the isomers in all three isotopes in Figs. 2, 3, and 4, suggest similarities in the level densities and the spin and parity distribution in the continuum of states that feed these states. The similar underlying nuclear structure from the odd proton occupying the $h_{11/2}$ orbital is also required. Similar level densities and spin and parity distributions are expected for high-spin states whose population can only come from a few high-spin states at greater excitation energy. This observation requires extensive nuclear modeling work in order to be quantified, and lies beyond the scope of the present work.

We note that in the lighter odd-mass Au and Ir isotopes the low-spin nuclear structure is known to be very similar in ^{189,191,193}Ir [5] and in ^{191,193,195,197}Au [6], while at lower masses the intruder $5/2^-$ and $9/2^-$ states change the order of low-spin levels. Assuming that the level densities and the spin and parity distribution in the continuum of states do not change drastically in ^{191,193,195,197}Au and ^{189,191,193}Ir a similar behavior in the feeding of the $11/2^-$ states in all these isotopes can be expected.

VI. SUMMARY

In conclusion, partial ^{191}Ir$(n,n'\gamma)^{191}$Ir^{m}, ^{193}Ir$(n,n'\gamma)^{193}$Ir^{m}, and ^{197}Au$(n,n')^{197}$Au^{m} cross sections for four γ-ray transitions for each target have been measured for neutron energies in the range $0.3 < E_n$ (MeV) < 20. A comparison of the population of the $11/2^-$ isomers was made. Striking similarities in the excitation functions of the corresponding transitions were observed, suggesting similarities in the level densities in the continuum that feeds the isomers, and confirming the similar underlying nuclear structure. The feeding of the isomers relative to the feeding of the corresponding ground states increases with increasing neutron energy up to $E_n \sim 10$ MeV. Above this neutron energy the opening of the $(n,2n)$ reaction channel affects more the population of the isomers and leads to a decrease of their relative population. Reasonable agreement between experiment and theoretical predictions from the FKK-GNASH reaction models was observed. Taken in combination with the observations of Ref. [15], these results provide further evidence for the use of different spin distributions for the pre-equilibrium and compound-nucleus portions of the reaction. The level density parameter does not require "tuning" from its recommended value as has often been suggested in work on isomer ratios.

ACKNOWLEDGMENTS

This work was performed under the auspices of the US Department of Energy (DOE) in part by the University of California, Los Alamos National Laboratory under Contract No. W-7405-ENG-36, and in part by Los Alamos National Security, LLC, Los Alamos National Laboratory under Contract No. DE-AC52-06NA25396, and in part by the University of California, Lawrence Livermore National Laboratory under Contract W-7405-ENG-48 and in part by Livermore National Security, LLC, Lawrence Livermore National Laboratory under Contract No. DE-AC52-07NA27344. This work has benefited from the use of the LANSCE accelerator facility supported under DOE Contract No. DE-AC52-06NA25396.

[1] E. Achterberg, O. A. Capurro, G. V. Marti, V. R. Vanin, and R. M. Castro, Nucl. Data Sheets **107**, 1 (2006).
[2] B. P. Bayhurst, J. S. Gilmore, R. J. Prestwood, J. B. Wilhelmy, N. Jarmie, B. H. Erkkila, and R. A. Hardekopf, Phys. Rev. C **12**, 451 (1975).
[3] V. R. Vanin, N. L. Maidana, R. M. Castro, E. Achterberg, O. A. Capurro, and G. V. Marti, Nucl. Data Sheets **108**, 2393 (2007).
[4] X. Huang and C. Zhou, Nucl. Data Sheets **104**, 283 (2005).
[5] B. Roussière *et al.*, Phys. At. Nucl. **64**, 1048 (2001), and references therein; Yad. Fiz. **64**, 1123 (2001).
[6] N. Fotiades, R. O. Nelson, M. Devlin, K. Starosta, J. A. Becker, L. A. Bernstein, P. E. Garrett, and W. Younes, Phys. Rev. C **71**, 064314 (2005).
[7] D. C. Larson, in *Proceedings of the International Conference on Nuclear Data for Basic and Applied Science, Santa Fe, New Mexico, USA, May 13–17* (Gordon and Breach Science Publishers, Inc., 1985), Vol. 1, p. 71.
[8] H. Vonach, A. Pavlik, M. B. Chadwick, R. C. Haight, R. O. Nelson, S. A. Wender, and P. G. Young, Phys. Rev. C **50**, 1952 (1994).
[9] J. A. Becker and R. O. Nelson, Nuclear Physics News International **7**, 11 (1997).
[10] A. Pavlik, H. Hitzenberger-Schauer, H. Vonach, M. B. Chadwick, R. C. Haight, R. O. Nelson, and P. G. Young, Phys. Rev. C **57**, 2416 (1998).
[11] L. A. Bernstein, J. A. Becker, W. Younes, D. E. Archer, K. Hauschild, G. D. Johns, R. O. Nelson, W. S. Wilburn, and D. M. Drake, Phys. Rev. C **57**, R2799 (1998).
[12] E. Tavukcu, L. A. Bernstein, K. Hauschild, J. A. Becker, P. E. Garrett, C. A. McGrath, D. P. McNabb, W. Younes, M. B. Chadwick, R. O. Nelson, G. D. Johns, and G. E. Mitchell, Phys. Rev. C **64**, 054614 (2001).
[13] E. Tavukcu, L. A. Bernstein, K. Hauschild, J. A. Becker, P. E. Garrett, C. A. McGrath, D. P. McNabb, W. Younes, P. Navratil, R. O. Nelson, G. D. Johns, G. E. Mitchell, and J. A. Cizewski, Phys. Rev. C **65**, 064309 (2002).
[14] D. Dashdorj, G. E. Mitchell, J. A. Becker, U. Agvaanluvsan, L. A. Bernstein, W. Younes, P. E. Garrett, M. B. Chadwick, M. Devlin, N. Fotiades, T. Kawano, and R. O. Nelson, Nucl. Sci. Eng. **157**, 65 (2007).
[15] D. Dashdorj, T. Kawano, P. E. Garrett, J. A. Becker, U. Agvaanluvsan, L. A. Bernstein, M. B. Chadwick, M. Devlin, N. Fotiades, G. E. Mitchell, R. O. Nelson, and W. Younes, Phys. Rev. C **75**, 054612 (2007).
[16] P. E. Garrett, L. A. Bernstein, J. A. Becker, K. Hauschild, C. A. McGrath, D. P. McNabb, W. Younes, E. Tavukcu, G. D. Johns, R. O. Nelson, W. S. Wilburn, and S. W. Yates, Phys. Rev. C **62**, 014307 (2000).
[17] P. E. Garrett, L. A. Bernstein, J. A. Becker, K. Hauschild, C. A. McGrath, D. P. McNabb, W. Younes, M. B. Chadwick, G. D. Johns, R. O. Nelson, W. S. Wilburn, E. Tavukcu, and S. W. Yates, Phys. Rev. C **62**, 054608 (2000).
[18] P. E. Garrett, J. A. Becker, L. A. Bernstein, W. E. Ormand, W. Younes, R. O. Nelson, M. Devlin, and N. Fotiades, Bull. Am. Phys. Soc. **47** No. 2, 161 (2002).
[19] P. E. Garrett, W. Younes, J. A. Becker, L. A. Bernstein, E. M. Baum, D. P. DiPrete, R. A. Gatenby, E. L. Johnson, C. A. McGrath, S. W. Yates, M. Devlin, N. Fotiades, R. O. Nelson, and B. A. Brown, Phys. Rev. C **68**, 024312 (2003).
[20] D. Dashdorj, G. E. Mitchell, T. Kawano, J. A. Becker, U. Agvaanluvsan, M. B. Chadwick, J. R. Cooper, M. Devlin, N. Fotiades, P. E. Garrett, R. O. Nelson, C. Y. Wu, and W. Younes, Nucl. Instrum. Methods Phys. Res. B **261**, 948 (2007).

[21] L. A. Bernstein, J. A. Becker, P. E. Garrett, W. Younes, D. P. McNabb, D. E. Archer, C. A. McGrath, H. Chen, W. E. Ormand, M. A. Stoyer, R. O. Nelson, M. B. Chadwick, G. D. Johns, W. S. Wilburn, M. Devlin, D. M. Drake, and P. G. Young, Phys. Rev. C **65**, 021601(R) (2002).

[22] N. Fotiades, G. D. Johns, R. O. Nelson, M. B. Chadwick, M. Devlin, W. S. Wilburn, P. G. Young, J. A. Becker, D. E. Archer, L. A. Bernstein, P. E. Garrett, C. A. McGrath, D. P. McNabb, and W. Younes, Phys. Rev. C **69**, 024601 (2004).

[23] W. Younes, J. A. Becker, L. A. Bernstein, P. E. Garrett, C. A. McGrath, D. P. McNabb, R. O. Nelson, M. Devlin, N. Fotiades, and G. D. Johns, UCRL ID-140313, Lawrence Livermore National Laboratory (2000).

[24] F. S. Stephens, in *Proceedings of the International Symposium on In-Beam Nuclear Spectroscopy* (Debrecen, Hungary, 1984), p. 205.

[25] P. W. Lisowski, C. D. Bowman, G. J. Russell, and S. A. Wender, Nucl. Sci. Eng. **106**, 208 (1990).

[26] N. Fotiades, R. O. Nelson, M. Devlin, M. B. Chadwick, P. Talou, J. A. Becker, P. E. Garrett, and W. Younes, AIP Conf. Proc. **769**, 898 (2005).

[27] R. O. Nelson, N. Fotiades, M. Devlin, J. A. Becker, P. E. Garrett, and W. Younes, in [26], p. 838, and references therein.

[28] S. A. Wender, S. Balestrini, A. Brown, R. C. Haight, C. M. Laymon, T. M. Lee, P. W. Lisowski, W. McCorkle, R. O. Nelson, and W. Parker, Nucl. Instrum. Methods Phys. Res. A **336**, 226 (1993).

[29] MCNPX User's Manual, version 2.6.0, edited by D. B. Pelowitz, Los Alamos National Laboratory Controlled Publication LA-CP-07-1473 (2007).

[30] R. O. Nelson, M. B. Chadwick, A. Michaudon, and P. G. Young, Nucl. Sci. Eng. **138**, 105 (2001).

[31] P. G. Young, E. D. Arthur, and M. B. Chadwick, in *Proceedings of the IAEA Workshop on Nuclear Reaction Data and Nuclear Reactors—Physics, Design and Safety, Trieste, Italy, April 15–May 17, 1996*, edited by A. Gandini and G. Reffo (World Scientific Publishing, Ltd., Singapore, 1998), pp. 227–404; Los Alamos National Laboratory report No. LA-UR-96-3739 (1996).

[32] H. Feshbach, A. Kerman, and S. Koonin, Ann. Phys. (NY) **125**, 429 (1980).

[33] P. Talou, T. Kawano, S. Cowell, M. B. Chadwick, H. Trellue, R. Nelson, and N. Fotiades, Los Alamos National Laboratory report No. LA-UR-06-4956 (2006).

[34] T. Kawano, P. Talou, and M. Chadwick, Nucl. Instrum. Methods Phys. Res. A **562**, 774 (2006).

[35] J. P. Delaroche, in *Proceedings of the International Conference on Neutron Physics for Reactors, Harwell, UK* (OCDE/Nuclear Energy Agency, Paris, 1978).

[36] J. Kopecky and M. Uhl, Phys. Rev. C **41**, 1941 (1990).

[37] A. V. Ignatyuk, G. N. Smirenkin, and A. S. Tishin, Sov. J. Nucl. Phys. **21**, 255 (1975).

[38] P. A. Moldauer, Phys. Rev. C **14**, 764 (1976).

[39] M. Blann and M. B. Chadwick, Phys. Rev. C **57**, 233 (1998).

[40] A. Gilbert and A. G. W. Cameron, Can. J. Phys. **43**, 1446 (1965).

[41] J. H. D. Jensen and J. M. Luttinger, Phys. Rev. **86**, 907 (1952).

[42] W. Dilg, W. Schantl, H. Vonach, and M. Uhl, Nucl. Phys. **A217**, 269 (1973).

[43] Reference Input Parameter Library, RIPL-2, Section 6, Nuclear Level Densities A. Ignatyuk and R. Capote, Coordinators, IAEA-TECDOC, International Atomic Energy Agency (2004).

[44] S. I. Al-Quraishi, S. M. Grimes, T. N. Massey, and D. A. Resler, Phys. Rev. C **67**, 015803 (2003).

[45] S. F. Mughabghab and C. Dunford, Phys. Rev. Lett. **81**, 4083 (1998).

[46] T. Kawano, S. Chiba, and H. Koura, J. Nucl. Sci. Technol. **43**, 1 (2006).

[47] S. Sudár and S. M. Qaim, Phys. Rev. C **73**, 034613 (2006).

[48] M. Al-Abyad, S. Sudár, M. N. H. Comsan, and S. M. Qaim, Phys. Rev. C **73**, 064608 (2006).

[49] N. Fotiades, R. O. Nelson, M. Devlin, M. B. Chadwick, P. Talou, J. A. Becker, L. A. Bernstein, P. E. Garrett, and W. Younes, Bull. Am. Phys. Soc. **48** No. 8, 42 (2003).

[50] P. Talou, M. B. Chadwick, R. O. Nelson, N. Fotiades, M. Devlin, P. E. Garrett, W. Younes, and J. A. Becker, in *Proceedings of the 10th International Conference on Nuclear Reaction Mechanisms, Varenna, June 9–13*, edited by E Gadioli (Ricerca Scientifica ed Educazione Permanente, 2003), p. 339.

[51] M. B. Chadwick, S. Frankle, H. Trellue, P. Talou, T. Kawano, P. G. Young, R. E. MacFarlane, and C. W. Wilkerson, Nucl. Data Sheets **108**, 2716 (2007).